

# Continuous Solar Observations from the Ground – Assessing Duty Cycle from GONG Observations

Kiran Jain, Sushant C. Tripathy, Frank Hill & Alexei A.  
Pevtsov

National Solar Observatory, 3665 Discovery Dr., Boulder, CO 80303, USA

E-mail: [kjain@nso.edu](mailto:kjain@nso.edu)

**Abstract.** Continuous observations play an important role in the studies of solar variability. While such observations can be achieved from space with almost 100% duty cycle, it is difficult to accomplish very high duty cycle from the ground. In this context, we assess the duty cycle that has been achieved from the ground by analyzing the observations of a six station network of identical instruments, Global Oscillation Network Group (GONG). We provide a detailed analysis of the duty cycle using GONG observations spanning over 18 years. We also discuss duty cycle of individual sites and point out various factors that may impact individual site or network duty cycle. The mean duty cycle of the network is 93%, however it reduces by about 5% after all images pass through the stringent quality-control checks. The standard deviations in monthly and yearly duty cycle values are found to be 1.9% and 2.2%, respectively. These results provide a baseline that can be used in the planning of future ground-based networks.

*Keywords:* Sun – helioseismology – *methods:* data analysis – *methods:* observational – *methods:* statistical

Submitted to: *Pub. Astron. Soc. Pacific*

## 1. Introduction

Solar observations are now available for a few centuries, however most of the records prior to the 20<sup>th</sup> century are sparse. The coverage has significantly increased in last few decades, primarily due to the advancement in observing capabilities from both space and ground. While observations from space are almost continuous with small disruptions, the ground-based observations are adversely affected by the diurnal cycle. There are several research areas in solar physics where uninterrupted observations for a long time are essential in order to achieve reliable results. Helioseismology is among one of these areas where solar oscillations below the surface are used to study phenomena occurring in the interior. These oscillations with a prominent period of 5-minutes were discovered in early 1960s (Leighton 1960, Leighton et al. 1962) and the physical mechanism explaining these observations was suggested about a decade later (Ulrich 1970, Leibacher & Stein 1971). It was soon realized that the continuous observations at high cadence for a longer time would be needed to reduce side lobes in the temporal power spectra, but this was not possible from a single ground station due to the diurnal cycle. There were two possibilities for continuous observations from ground: either from the South Pole but for a limited time during the Austral Summer (Grec et al. 1980) or build a network of identical instruments at geographically separated locations around the Earth. This led to the inception of several networks for helioseismic observations; some are still operational even after more than 25 years and other ceased operations after a few years. Observations from these networks allowed the measurement of solar oscillations from low to high degrees where degree is the number of waves around the solar circumference.

Some of the short-lived networks were the *International Research on the Interior of the Sun* (Fossat 1991, IRIS) and the *Taiwanese Oscillations Network* (Chou et al. 1995, TON). Two still operating networks are the *Birmingham Solar Oscillation Network* (Chaplin et al. 1996, BISON) since 1975 and the *Global Oscillation Network Group* (Leibacher & GONG Project Team 1995, GONG) since 1995. While BiSON provides observations in solar-disk-integrated light best suitable for low spherical harmonic degree helioseismic modes, which travel deep into the core, GONG observations resolve acoustic modes covering a wider range from core to the near-surface layers. In addition, several observational campaigns were held at the South Pole from the early 1980s to mid-1990s (Harvey 2013, Fossat 2013), however continuous observations were obtained for a maximum period of about a week. Occasional observation campaigns at the South Pole are still continuing with specific science goals (Finsterle et al. 2004, Jefferies et al. 2019) but continuous observations were acquired only for a few days. All of these observations played a crucial role in advancing the research in helioseismology and confirmed the solar variability below the surface as observed above the surface, first reported by Woodard & Noyes (1985). Furthermore, observations from the current or past space missions also complemented the ground-based observations (Pallé et al. 2015).

In this article, we assess the temporal coverage from the ground-based observatories using observations of the GONG network. Section 2 presents a brief history of GONG.

**Table 1.** Locations of GONG sites and operation start dates.

Site		Latitude	Longitude	Elevation [meters]
Name	Identifier			
Learmonth, Australia	LE	S 022° 13' 06.6"	E 114° 06' 09.8"	15
Udaipur, India	UD	N 024° 36' 53.8"	E 073° 40' 10.9"	677
El Teide, Spain	TD	N 028° 18' 03.0"	W 016° 30' 43.0"	2425
Cerro Tololo, Chile	CT	S 030° 10' 04.2"	W 070° 48' 19.7"	2190
Big Bear, USA	BB	N 034° 15' 37.2"	W 116° 55' 17.1"	2063
Mauna Loa, USA	ML	N 019° 32' 10.1"	W 155° 34' 33.3"	3471

**Figure 1.** Locations of GONG sites around the world.

Data used to compute duty cycle is described in Section 3. Assessment of the duty cycle of individual sites and the network as a whole are discussed in Sections 4 and 5, respectively. We also provide statistical analysis of the simultaneous observations between different sites in 6. Section 7 demonstrates the scientific need of high duty cycle, especially in helioseismic studies. Finally, the summary is presented in Section 8.

## 2. A Brief History of GONG: From Helioseismology to Space Weather

One of the first tasks in establishing a network of observatories is to identify the number and locations of the sites suitable for substantially reducing the observed diurnal cycle. For this, a systematic study of potential sites for the GONG network started with estimating the performance of several hypothetical ground-based network composed of two to six existing observing sites distributed in both longitude and latitude. Results suggested that a network of six sites was needed to achieve  $> 90\%$  annual mean duty cycle (Hill & Newkirk 1985). This initiated a coordinated site survey with identical instruments (Fischer et al. 1986) placed at 15 sites around the globe, divided into six longitudinal bands to measure the cloud-cover percentage and transparency of the sky. Based on the detailed analysis of the collected data (Hill, Fischer, Grier, Leibacher, Jones, Jones, Kupke & Stebbins 1994) and the overall performance of

each site (Hill, Fischer, Forgach, Grier, Leibacher, Jones, Jones, Kupke, Stebbins, Clay, Ingram, Libbrecht, Zirin, Ulrichi, Websteri, Hieda, Labonte, Lu, Sousa, Garcia, Yasukawa, Kennewell, Cole, Zhen, Su-Min, Bhatnagar, Ambastha, Al-Khashlan, Abdul-Samad, Benkhaldoun, Kadiri, Sánchez, Pallé, Duhalde, Solis, Saá & González 1994), six sites were finally selected in early 1991. Each selected site represents one of the six longitudinal bands that allows the network to make 24-hour-a-day observations of the Sun year round. These sites are shown in Figure 1 and their locations are given in Table 1.

The GONG instrument is based on measuring the line-of-sight Doppler shifts of the photospheric spectral line Ni I 676.8 nm. The key element of this instrument is a Michelson interferometer, the details of which are given by (Harvey & GONG Instrument Team 1995). Deployment of the GONG instruments started in January 1995 with the TD site and the full network was completed in October of the same year after UD, the last site, became operational. Start dates of the operations at each site are also given in Table 1. Identical instruments and identical settings at all six sites operating in automated mode with minimal human intervention is the key to the network’s success. The science-grade data of the network are available since 7 May 1995. At the beginning, the observations were carried out with low-resolution cameras that had rectangular pixels (aspect ratio of 1.28:1) and was oriented in such a way that the longer dimension was aligned with the solar axis of rotation. The resulting images were  $204 \times 239$  pixels across with a pixel resolution of  $\approx 10 \times 8$  arcseconds.

After observing successfully for the initial three years using low-resolution cameras (Harvey et al. 1996), the capabilities of the GONG network were expanded in 2001 by upgrading its cameras to  $1024 \times 1024$  with square pixels (Harvey et al. 1998). Until 2001, the GONG, commonly known as GONG classic, data usage was primarily limited to global helioseismic studies. The upgrade provided data that is suitable for local helioseismic studies, e.g. internal conditions below small regions on the surface, hemispheric and latitudinal distributions of subsurface flows, mapping of the farside for the detection of active regions, etc. The upgraded network is commonly referred to as GONG+. This also served as the starting point to expand GONG’s capabilities to space weather. In subsequent years, the GONG observations were extended to one-minute cadence full-disk magnetograms in 2006 (Petrie et al. 2008, Hill et al. 2008) and  $2048 \times 2048$  pixels images of the  $H\alpha$  spectral line at a wavelength of 656.28 nm in mid-2010 (Harvey et al. 2011). Note that all  $H\alpha$  observations are taken at a cadence of one minute at each site but with the acquisition time offset between adjacent sites so that a new  $H\alpha$  image is, in principle, available every 20 seconds from the network. Various GONG data products are available at <https://nso.edu/data/nisp-data/>, and their applications in space-weather related studies and predictions are described by (Hill 2018).

**Table 2.** Details of the network data used in this study.

Data Type	Count	Duty Cycle	Details
Period covered	18 years (2002–2019)		
Total Number of days	6574		
Total Minutes covered	$9.47 \times 10^6$		
Total Observations from all sites	$1.35 \times 10^7$		
Total Minutes with observations	$8.36 \times 10^6$	88.33 %	
Total Minutes with no observations	$1.11 \times 10^6$	11.67 %	
Total minutes with independent observations	$4.12 \times 10^6$	43.49 %	Table 3
Total minutes with simultaneous observations	$4.24 \times 10^6$	44.84 %	Table 4

### 3. Data

We compute the duty cycle of individual sites or the network from *fully calibrated images* that have successfully passed through stringent quality checks as described in the Automated Image Rejection (Clark et al. 2004, AIR), and consist of, for example, active tracking, image stability, signal/noise level in individual images (Toussaint et al. 1995, Pintar & Toussaint 1998), temporal variations between images, and the correction for orientation for the best position-angle estimation (Toner 2001). As mentioned in Section 2, GONG has many different observables out of which we choose observations of Doppler velocities to determine the duty cycle. While the magnetograms and the Dopplergrams are part of the same observing sequence, the data products go through different processing pipelines and thus have different image rejection criteria as part of the quality control. H $\alpha$  observations have been taken since 2010 using a different instrument setup and may provide a slightly different duty cycle.

The duty cycle is defined as the fraction of 24-hour day for which the observations are available. In addition, the network duty cycle is determined by combining all six site images for each minute in the same 24-hour period. There are several factors that significantly influence the observations at individual sites and, finally, the network duty cycle. These factors include, but are not limited to, severe weather conditions, instrument problems, downtime due to preventive maintenance and upgrades, etc. Although the network has been operational for more than 25 years, we consider only a period of 18 years from January 2002 to December 2019 for assessing the duty cycle, i.e. the period after the completion of camera upgrade. This period allows us to analyze consistent data set without any forced major disruptions. A total number of 6574 days, i.e.  $9.47 \times 10^6$  minutes, are covered in this study. Since there are overlapping observations between different sites and GONG provides observations at a cadence of one minute, the analysis has been carried out using more than 13 million images collected at GONG sites over the period of 18 years. Tables 2 summarizes the details of the network input

**Table 3.** Details of individual site data used in this study.

Sites	Contribution to total observations	Contribution to network duty cycle		
		Total	Independent	Overlapping
LE	18.6 %	26.6 %	12.9 %	13.7 %
UD	11.2 %	15.9 %	5.1 %	10.8 %
TD	17.8 %	25.7 %	8.7 %	17.0 %
CT	21.1 %	30.1 %	8.0 %	22.1 %
BB	16.5 %	23.6 %	4.7 %	18.9 %
ML	14.8 %	21.2 %	4.1 %	17.1 %

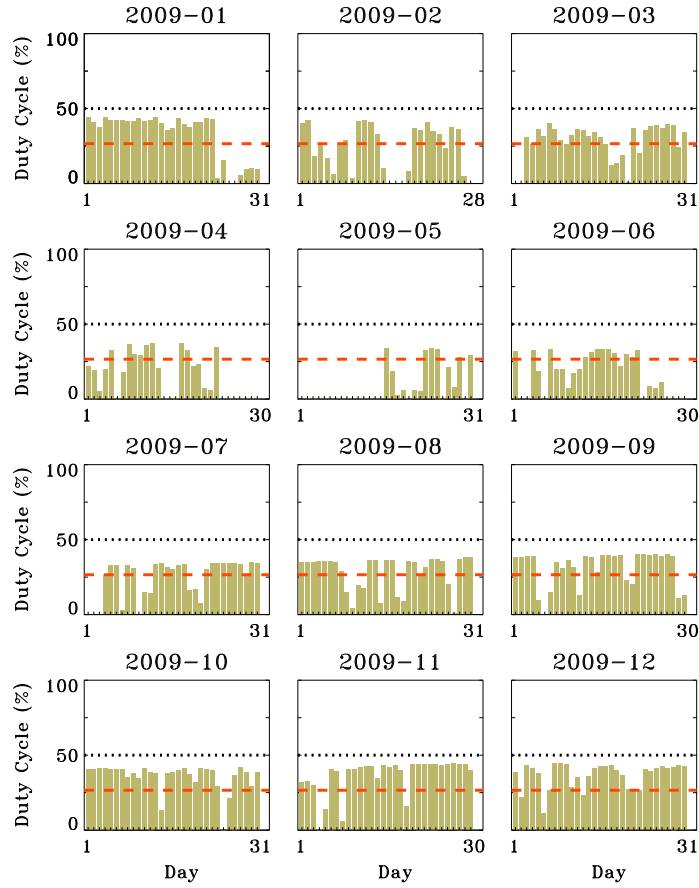
data and Table 3 provides the details of each site’s data. In the next section, we describe the performance of individual sites starting from the East. Results for the full network are discussed in Section 5.

## 4. Individual Site Duty Cycle

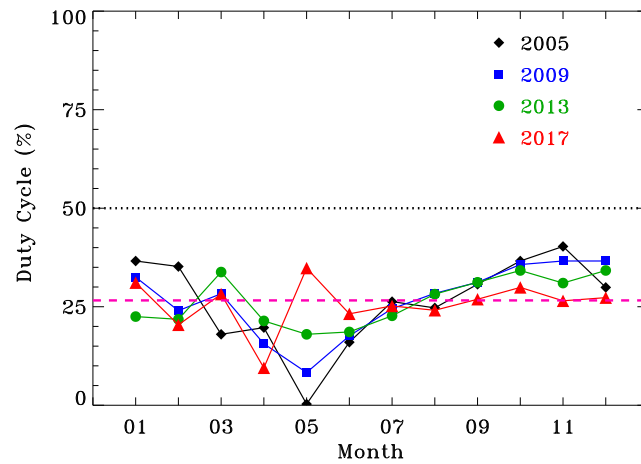
### 4.1. Learmonth, Australia (LE)

The Learmonth Solar Observatory (LSO) situated on the western shore of the Exmouth Gulf on the North West Cape of Australia houses one of GONG’s instruments. The observatory is co-administered by the Bureau of Meteorology, Australian Government, and the US Air Force. This GONG site became operational in April 1995. We display the variation of daily duty cycle in Figure 2, as an example, for the year 2009. Here different panels represent different calendar months. In addition to the seasonal variation in duty cycle, there are some random gaps, which signify no observations for entire days. Longer gaps (e.g. from the last week of April to mid-May in Figure 2) generally arise due to instrument downtime or preventive maintenance periods while shorter gaps correspond to severe weather that may last from one to a few days. The maximum daily observations were obtained for 11.47 hours which gives a duty cycle of 47.8 %. In total, LE provided observations for 5621 days out of 6574 days (i.e. 85.5 % days). Various milestones achieved by individual sites are given in Table 4.

To examine the trends in LE observations, we display in Figure 3 the monthly variation in duty cycle for four selected years. A systematic seasonal variation is seen in all four years with a dip in the duty cycle in April–May, except for 2017, followed by an increasing trend. The higher duty cycle is achieved in later months every year with the beginning of Summer in the southern hemisphere due to the availability of sunshine over a larger fraction of the day. The overall trends in monthly and yearly variations averaged over the entire period are presented in Figures 4 and 5, respectively. We have included other GONG sites in the same figure for comparison. As mentioned above, the trend in the mean monthly values display strong seasonal variation with a standard deviation of 6.0 %. When we consider yearly variation (see Figure 5), LE’s contribution to the GONG network has been stable throughout the entire period and, as a result,



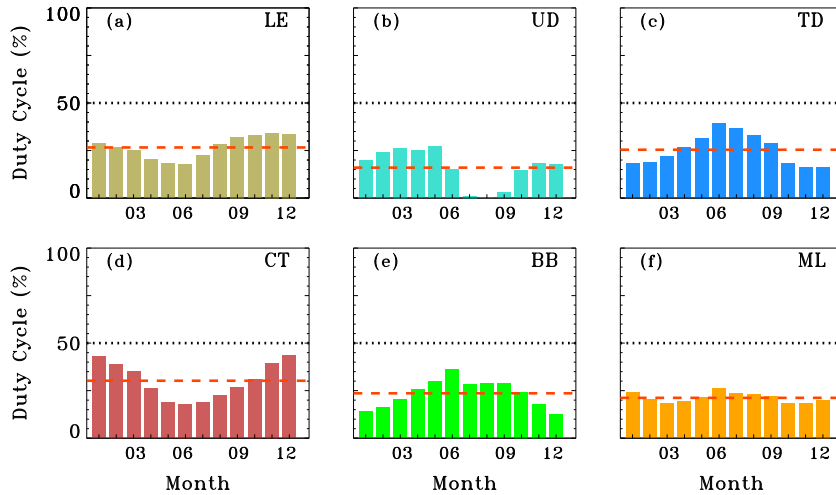
**Figure 2.** Daily duty cycle for Learmonth (LE) site for each month in the year 2009. The dashed (red) line represents the mean value over the entire period (see Table 4) whereas the dotted (black) line shows a duty cycle value of 50 %.



**Figure 3.** Monthly duty cycle for Learmonth (LE) site for selected years. Yearly means for 2005, 2009, 2013, and 2017 are 26 %, 27 %, 27 %, and 26 %, respectively. The dashed (pink) line represents the mean value over the entire period (see Table 4) whereas the dotted (black) line shows a duty cycle value of 50 %.

**Table 4.** Various performance figures achieved by individual sites.

Criterion	Frequency	LE	UD	TD	CT	BB	ML
Total coverage [Days]	All	5621	3949	5280	5516	5532	5536
Mean Duty Cycle [%]	All	26.6	16.0	25.4	30.2	23.6	21.2
Median Duty Cycle [%]	Monthly	28.2	18.4	26.5	31.1	25.5	21.4
	Yearly	26.5	16.2	25.7	31.1	23.8	21.1
Maximum Duty Cycle [%]	Daily	47.8	46.7	49.4	50.3	48.5	47.7
	Monthly	34.2	27.0	39.4	43.6	36.3	26.1
	Yearly	31.1	21.4	30.2	33.1	25.6	29.5
Minimum Duty Cycle [%]	Daily	0.0	0.0	0.0	0.0	0.0	0.0
	Monthly	17.8	4.0	16.1	18.0	12.6	18.1
	Yearly	23.1	9.9	20.5	26.4	19.8	14.1
Standard Deviation [%]	Monthly	6.0	9.7	8.3	9.7	7.3	2.6
	Yearly	2.0	3.0	2.6	2.2	1.4	3.3

**Figure 4.** Monthly variation in duty cycle averaged over the entire period for all six GONG sites. Horizontal dotted (black) and dashed (red) lines represent 50% and the mean value for individual sites over the entire period (see Table 4), respectively.

the standard deviation reduces to about 2.0%.

From Table 3, we find that the observations taken at LE contribute about 18.6% to the total observations and 26.6% to the network duty cycle. As mentioned earlier, all sites provide independent as well as overlapping observations and LE's contribution to the network duty cycle is almost equally split between these two categories. It is further noted that LE's independent contribution is the largest among all sites.



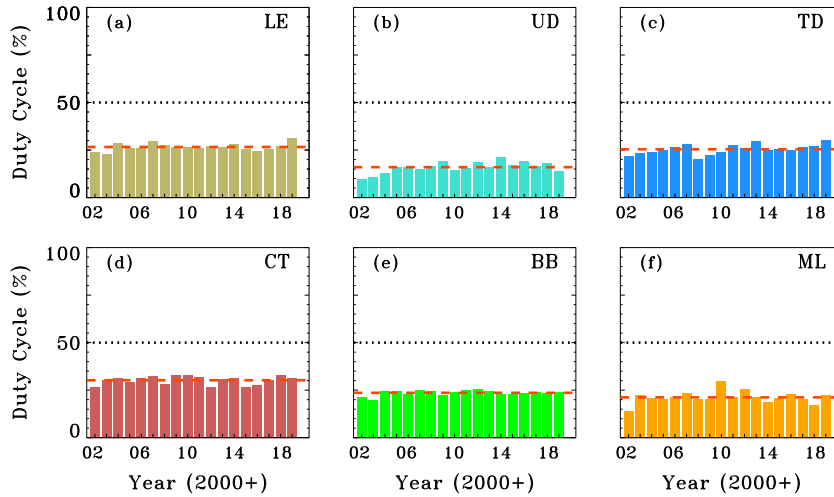


**Figure 5.** Yearly variation in duty cycle for all six GONG sites. Horizontal dotted (black) and dashed (red) lines represent 50% and the mean value for individual sites over the entire period (see Table 4), respectively.

#### 4.2. Udaipur, India (UD)

The Udaipur Solar Observatory (USO) is situated in a semi-arid highland region of Western India and houses the GONG’s instrument in the Asian band. USO is administered by the Physical Research Laboratory (Ahmedabad), a unit of Department of Space, Government of India. The Udaipur site experiences strong weather pattern with an extended period of monsoon lasting for two–three months every year and the observations are stopped during this period. As a result, UD’s contribution to the total observations is the lowest at 11.2%. As presented in Table 3, UD provides only 5.1% independent contribution to the network duty cycle while the total contribution is 15.9%. Two-thirds of UD observations have overlap with other sites and the details are given in Section 5.

To evaluate the daily variation throughout the year, we show daily duty cycle for the year 2009 in Figure 6 and the monthly duty cycle for four selected years in Figure 7. Compared to LE, Udaipur observations have many longer gaps in 2009. The UD site was down from early July to mid-September due to the monsoon and the other two gaps, in late January and early October, are due to system failures and occurrence of preventive maintenance. The downtime due to the monsoon is seen in all monthly average plots presented in Figure 7. The duty cycle again decreases in December–January due to hazy conditions and less sunshine hours available during Winter months. The maximum observations are normally obtained from February to May. During Spring/Summer time, the Udaipur site observed for more than 11 hours and the maximum daily duty cycle during 2002–2019 reached 46.7%.

The average monthly and yearly duty-cycle trends, as shown in Figures 4b and 5b, clearly demonstrate the effect of the monsoon on the duty cycle. The seasonal variation in mean duty cycle for UD is more significant than for LE. As a result, the

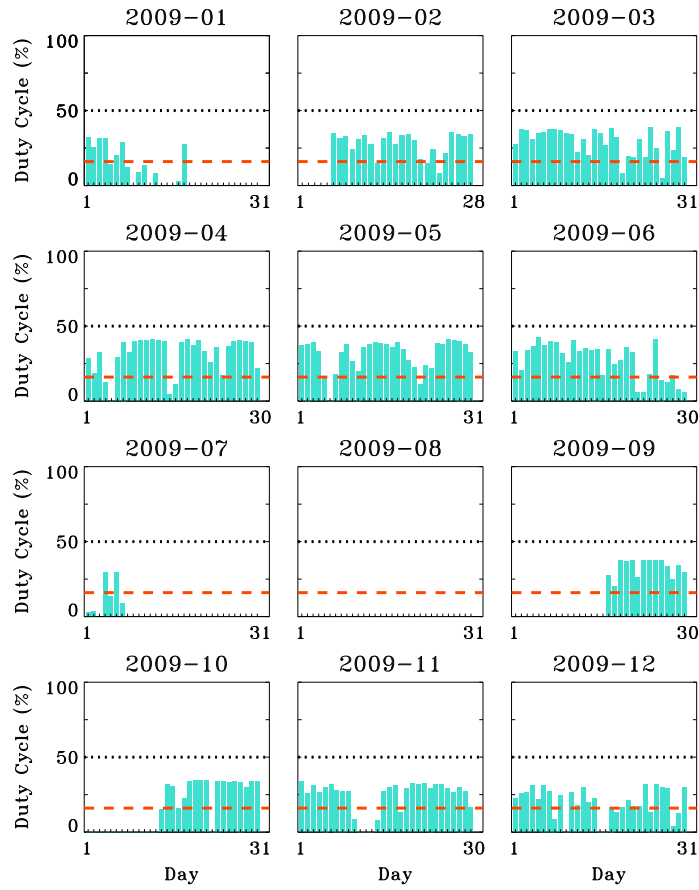


**Figure 6.** Daily duty cycle for Udaipur (UD) site for each month in the year 2009. The dashed (red) line represents the mean value over the entire period (see Table 4) whereas the dotted (black) line shows a duty cycle value of 50 %.

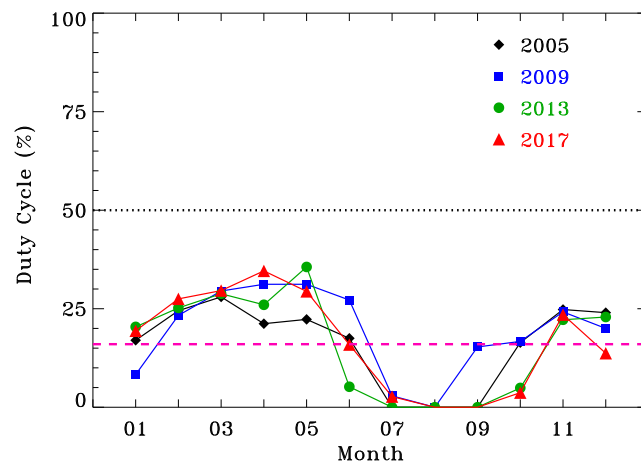


**Figure 7.** Monthly duty cycle for Udaipur (UD) site for selected years. Yearly means for 2005, 2009, 2013 and 2017 are 16 %, 19 %, 16 %, and 17 %, respectively. The dashed (pink) line represents the mean value over the entire period (see Table 4) whereas the dotted (black) line shows a duty cycle value of 50 %.

standard deviations, as summarized in Table 4, are also higher for both monthly and yearly averages. In addition, the mean duty cycle is notably lower. Total observations from UD are available for 60.1 % or 3949 days during the period of 18 years, the lowest among all sites. The lower coverage from UD was a combination of the monsoon season and several other long periods of system downtime, for example, a fire broke in the GONG instrument shelter in August 2010 and the site remained non-operational until the beginning of 2011.

#### 4.3. *El Teide, Canary Islands (TD)*

The El Teide site is located on the island of Tenerife, in the Canary Islands off the west coast of Africa, hosted by the Instituto Astrofísica de Canarias (IAC). The IAC is administered by a public consortium which includes the Universidad de la Laguna. Similar to other sites, observations from TD are also affected by strong seasonal variations. Sometimes it is hit by intense dust storm, known as the *Calima*, blowing off the Sahara Desert. During the *Calima*, strong winds are accompanied by a orange haze that significantly reduces the sky transparency and the observations, if any, are discarded. Even after being affected by the several months of poor weather conditions in Winter and Summer, TD provides a good coverage of about 80.3 % of the days.

The daily duty cycles for TD are presented in Figure 8 for 2009. It is evident that daily observations from TD are consistent for several months in Summer, thus providing good coverage to the GONG network. This is also apparent from Figure 9 where the duty cycle from April to September for all four years is consistently higher than other months. From Table 3, one can notice that TD's contribution to the network duty cycle is about 25 % which is similar to LE. The independent contribution from the Teide site is 8.7 % in the overall duty cycle. This site along with LE becomes notably more important when the UD instrument is down for the long monsoon season or any other down-time. During a clear day in Summer, good observations for almost 12 hours can be obtained from this site.

Similar to other sites, a strong weather-dependent variation in the TD duty cycle is apparent in Figures 4c where we show the monthly duty cycle averaged over the entire period considered in this study. It is noted that the duty cycle drops to almost one half in the Winter months and the standard deviation in the monthly mean duty cycle is moderately large with a value of 8.3 %. However, the yearly variation is relatively small (Figure 5c) with a standard deviation of only 2.6 % (Table 4).

#### 4.4. *Cerro Tololo, Chile (CT)*

The second GONG site in the southern hemisphere is located on the mountain Cerro Tololo in northern Chile. The instrument is located on the grounds of the Cerro Tololo Interamerican Observatory (CTIO), a division of NSF's National Optical-Infrared Astronomy Research Laboratory (NSF's NOIRLab) headquartered in Tucson, USA. Due to excellent sky conditions, CTIO is one of the main sites for astronomical investigations

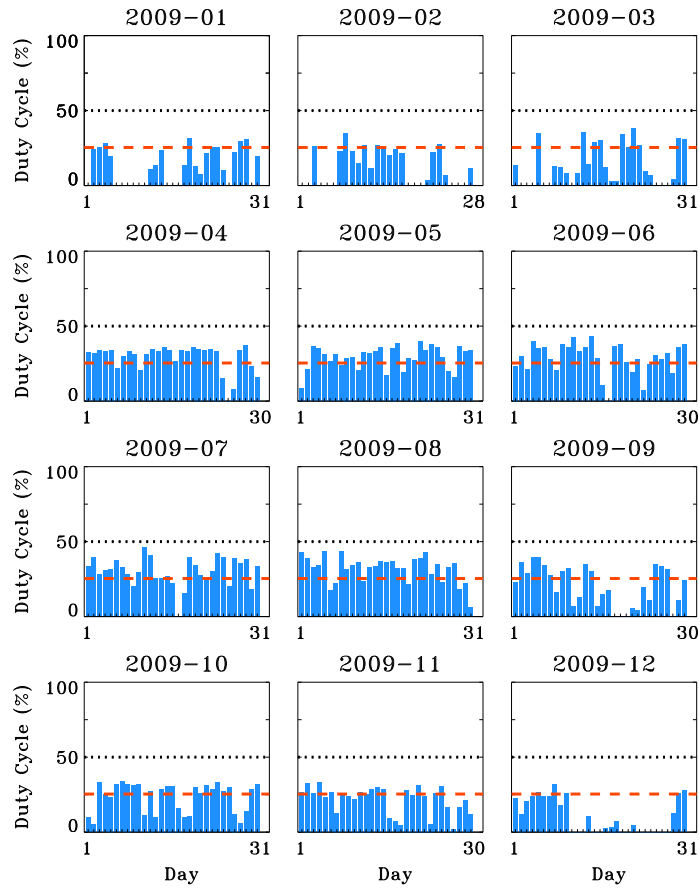


**Figure 8.** Daily duty cycle for the El Teide (TD) site for each month in 2009. The dashed (red) line represents the mean value over the entire period (see Table 4) whereas the dotted (black) line shows a duty cycle value of 50 %.

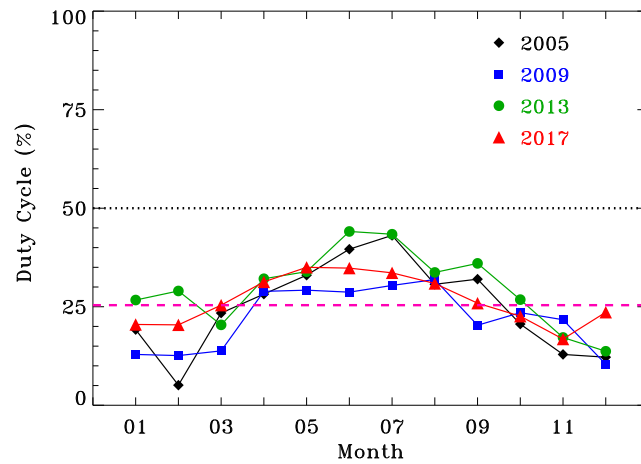


**Figure 9.** Monthly duty cycle for the Teide (TD) site for selected years. Yearly means for 2005, 2009, 2013, and 2017 are 25 %, 22 %, 30 %, and 27 %, respectively. The dashed (pink) line represents the mean value over the entire period (see Table 4) whereas the dotted (black) line shows a duty cycle value of 50 %.

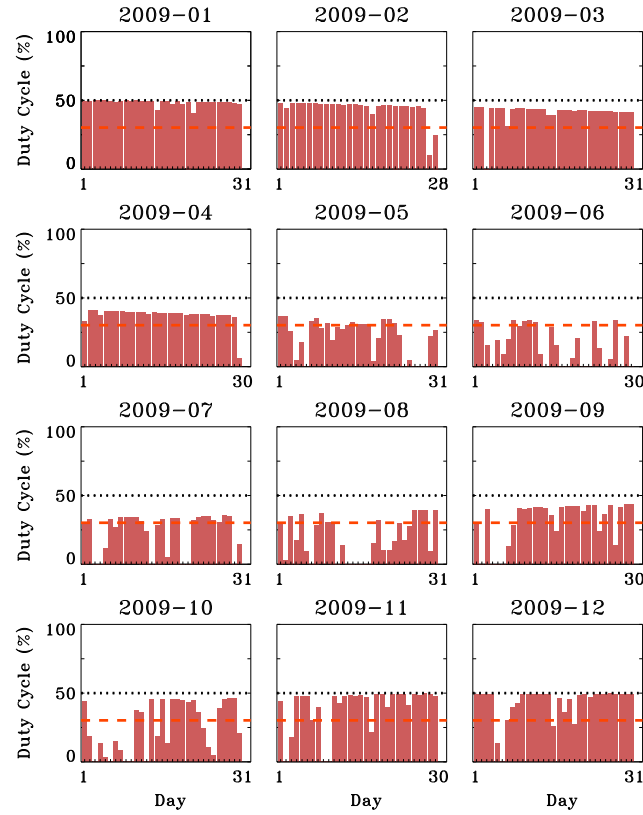


**Figure 10.** Daily duty cycle for Cerro Tololo (CT) site for each month in 2009. The dashed (red) line represents the mean value over the entire period (see Table 4) whereas the dotted (black) line shows a duty cycle value of 50 %.

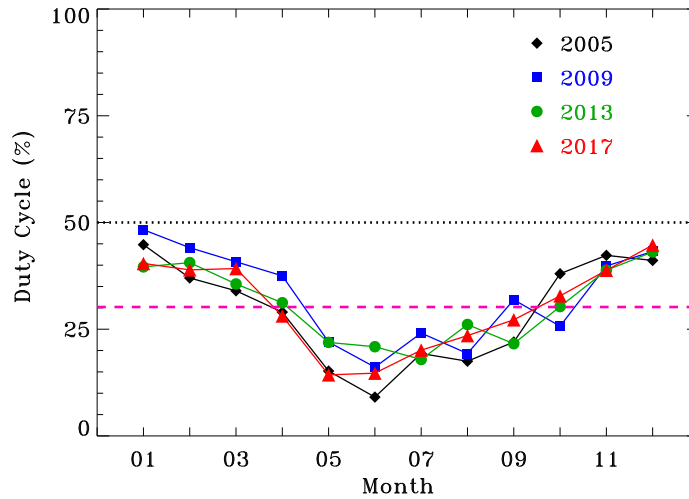


**Figure 11.** Monthly duty cycle for Cerro Tololo (CT) site for selected years. Yearly means for 2005, 2009, 2013, and 2017 are 29 %, 33 %, 31 %, and 30 %, respectively. The dashed (pink) line represents the mean value over the entire period (see Table 4) whereas the dotted (black) line shows a duty cycle value of 50 %.

of the southern skies. This is reflected in the number of observations from the individual sites summarized in Table 3. CT's contribution to GONG's cumulative observations is the highest and has 5516 observing days, that is about 84 % of the total days. Despite a significantly large number of observations and about 30 % contribution to the network duty cycle, the independent contribution from CT is only 8.0 % while overlapping observations cover the remaining 22.1 %, as evident from Table 3. This large fraction of overlapping observations are due to the proximity of adjacent sites BB and TD. Moreover, CT has the maximum overlap with the neighboring sites' observations.

Daily variation in duty cycles for the year 2009 is presented in Figure 10, which exhibits stability for several months. Maximum duty cycle of about 50 % is achievable for several months, i.e. January, February, November, and December. From the monthly variation for four sample years (Figure 11), it is clear that the number of observations from CT reaches its lowest value in the month of June. This strong seasonal variations is also noticeable in Figure 4d and the standard deviation in the monthly duty cycle is about 9.7 %. Aside from the seasonal variation, the yearly duty cycles from CT remain reasonably high as shown in Figure 5d and the values remain between 28 % – 33 % with a standard deviation of 2.2 %, as given in Table 4.

#### 4.5. *Big Bear, USA (BB)*

The only GONG site in the United States mainland is located in the southwest on the premises of Big Bear Solar Observatory (BBSO), managed by the New Jersey Institute of Technology (NJIT). The instrument is placed on the north shore of an artificial lake in the San Bernardino Mountains in California. Similar to other sites, BB also has strong seasonal variation in the duty cycle that peaks around June and reaches its lowest value in December – January. From the daily duty-cycle histograms, as shown in Figure 12, it is evident that the observations are sparse in the Winter months. Although the observations from BB are consistent in Summer months, there are a few years when the duty cycle is relatively low and 2009 is among those years. As illustrated in Figure 13, the monthly duty-cycles for four years clearly show the variation from one year to another. The overall trend is more pronounced in Figure 4e where the average monthly duty cycle is shown. A gradual increase in the duty cycle is observed after February with a maximum in June, a slow decrease during July to September and finally, a sharp decline is noticed until December.

We note that the Big Bear site has been very stable throughout the operations of GONG and the year-to-year variation is the least among all six GONG sites (See Figure 5e). Therefore, the standard deviation in yearly values is also a minimum, i.e. only 1.4 %, while the standard deviation in monthly values is 7.3 %. Table 4 shows that the observations collected at BB spanned over 5532 days that is about 84.1 % of the total observing days. The BB contribution to all GONG observations is around 16.5 % with three-quarters of them have overlap with other sites as described in Table 3. Nevertheless, the independent coverage of 4.7 % in total duty cycle makes this site

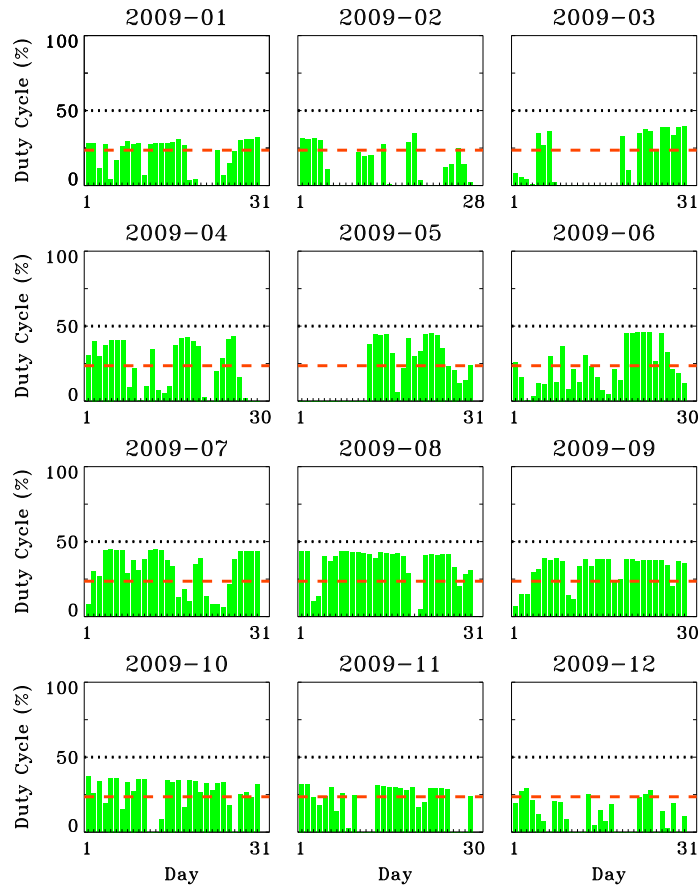


**Figure 12.** Daily duty cycle for Big Bear (BB) site for each month in the year 2009. The dashed (red) line represents the mean value over the entire period (see Table 4) whereas the dotted (black) line shows a duty cycle value of 50 %.

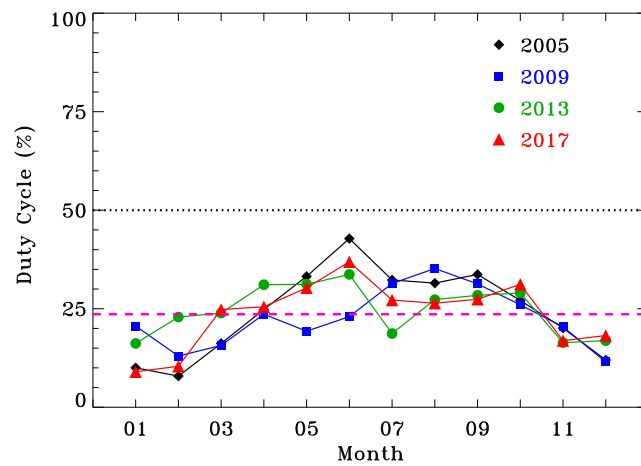


**Figure 13.** Monthly duty cycle for Big Bear (BB) site for selected years. Yearly means for 2005, 2009, 2013, and 2017 are 24 %, 23 %, 27 %, and 24 %, respectively. The dashed (pink) line represents the mean value over the entire period (see Table 4) whereas the dotted (black) line shows a duty cycle value of 50 %.

equally important with other GONG sites.

#### 4.6. Mauna Loa, USA (ML)

The sixth GONG site is located at the north side of the Mauna Loa volcano at the Mauna Loa Observatory (MLO), on the island of Hawai'i (Big Island). MLO is an atmospheric baseline station of the Global Monitoring Laboratory (GML) of the National Oceanic and Atmospheric Administration (NOAA). Local staff support is provided by the Mauna Loa Solar Observatory operated by the High Altitude Observatory, Boulder, Colorado. Unlike other GONG sites, Mauna Loa is minimally affected by strong seasonal variations. This is clearly visible in the daily duty-cycle plot for a year displayed in Figure 14. Although we do see variations from month to month, these are not as strong as in other sites and the daily values remain in a similar range throughout the year. Further, to evaluate the existence of this pattern in all years, we plot monthly values for four individual years in Figure 15. This shows no distinct trend in the monthly variation within a year, however there are random fluctuations, but these do not indicate any strong seasonal pattern. On averaging monthly values over the entire period presented in Figure 4f, a mild pattern emerges with minor dips around both equinoxes. Finally, we find that the standard deviation in monthly values for ML is only about 2.6 % which is the lowest among all sites ( Table 4). However, the standard deviation in yearly values displayed in Figure 5f is higher than the monthly value and also the highest among all sites indicating that ML experienced the highest year-to-year variation in the duty cycle.

In addition, the number of observing days at ML at 84.2 % level is comparable with CT and BB, but the contribution to the total network observations is the second lowest (see Table 3). It is worth pointing out that the independent observations from ML cover merely 4.1 % which is the lowest among all six sites; more than three-quarters of ML observations overlap with other sites.

### 5. Network Duty Cycle

Section 4 clearly demonstrates that all sites except ML are affected by strong seasonal patterns. While sites in the northern hemisphere provide good coverage during Summer months (humps in June–July for BB and TD in Figure 4), this trend reverses in the southern hemisphere (dips in June–July for LE and CT). Further, due to the low latitude location, the seasonal patterns are less apparent in ML observations. However, the network observations after integrating over those from individual sites (Toner et al. 2003) display a consistent coverage throughout the year with significantly high duty cycle. Figure 16 presents network daily duty cycle for a year exhibiting minimal weather-related patterns and the daily value reaches  $> 90\%$  in most cases. We do notice some days with duty cycles dipping down to 50 % or lower but these are rare. To better understand the variation, if any, we compute mean monthly duty cycles for



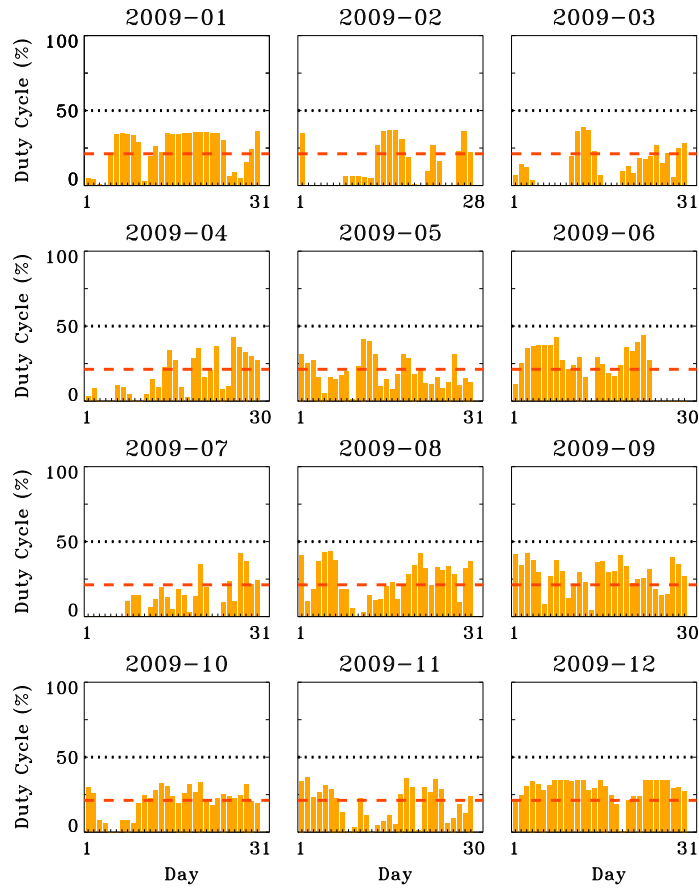


**Figure 14.** Daily duty cycle for Mauna Loa (ML) site for each month in 2009. The dashed (red) line represents the mean value over the entire period (see Table 4) whereas the dotted (black) line shows a duty cycle value of 50 %.

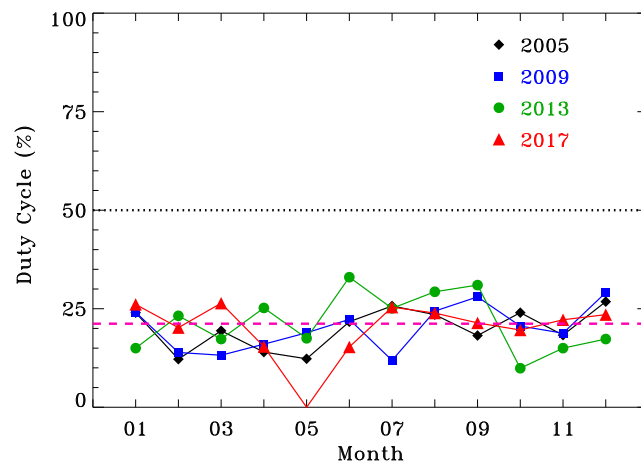


**Figure 15.** Monthly duty cycle for Mauna Loa (ML) site for selected years. Yearly means for 2005, 2009, 2013, and 2017 are 20 %, 20 %, 22 %, and 20 %, respectively. The dashed (pink) line represents the mean value over the entire period (see Table 4) whereas the dotted (black) line shows a duty cycle value of 50 %.

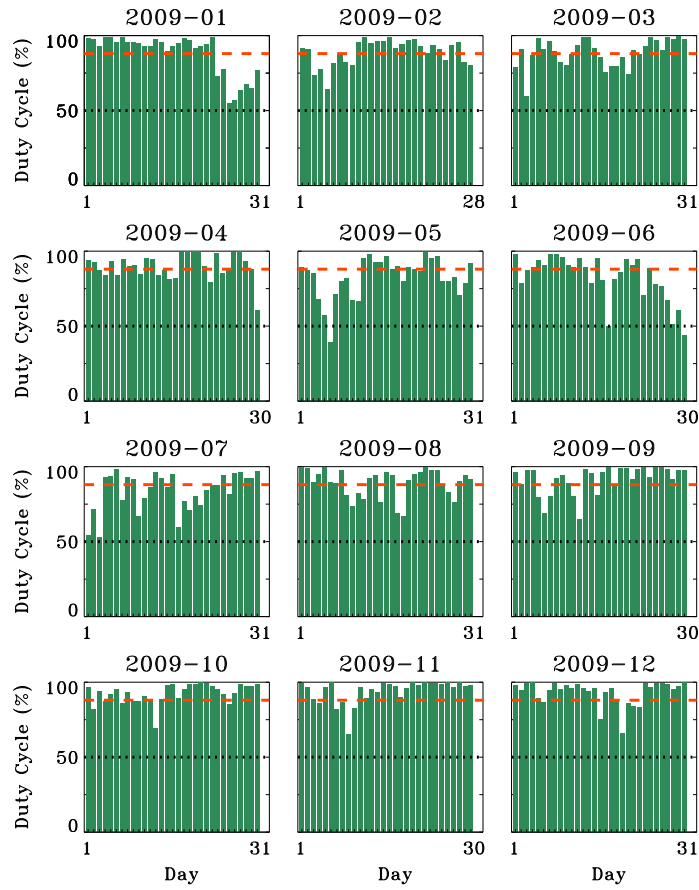


**Figure 16.** Daily duty cycle of the GONG network for 2009. The dashed (red) line represents the mean value over the entire period (see Table 2) whereas the dotted (black) line shows a duty cycle value of 50 %.

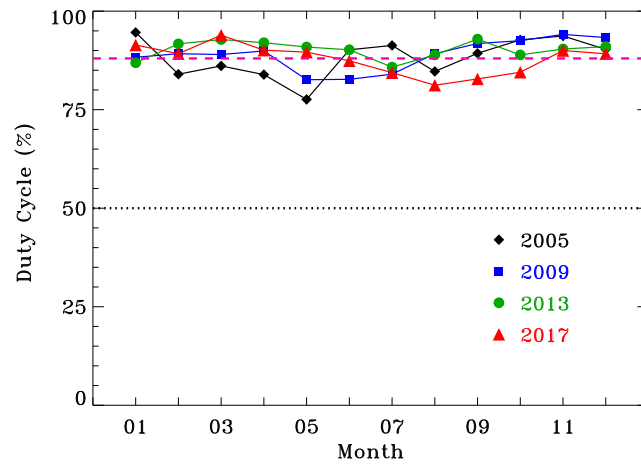


**Figure 17.** Mean monthly duty cycle of the GONG network for four selected years. Yearly means for 2005, 2009, 2013, and 2017 are 88 %, 89 %, 90 %, and 88 %, respectively. The dashed (pink) line represents the mean value over the entire period (see Table 2) whereas the dotted (black) line shows a duty cycle value of 50 %.

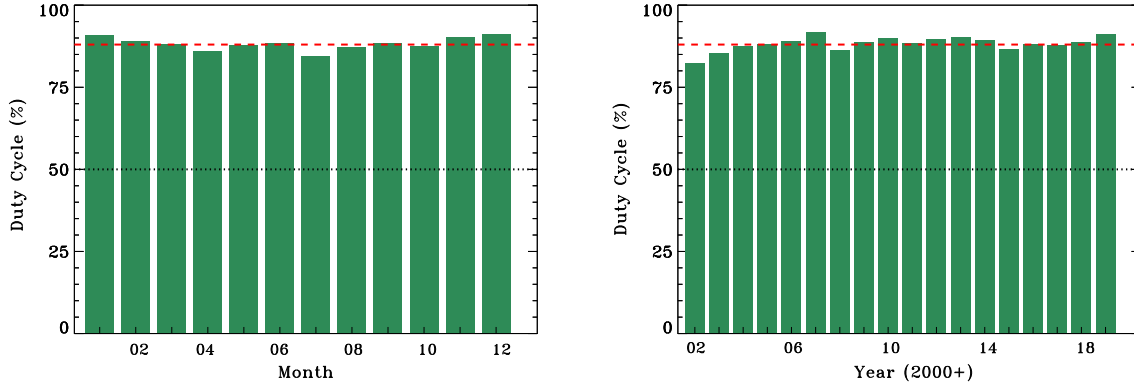


**Figure 18.** (Left) Monthly and (Right) yearly variations in the network duty cycles. The dashed (red) line represents the mean value over the entire period (see Table 2) whereas the dotted (black) line shows a duty cycle value of 50 %.

the network for four years and present them in Figure 17. We do not see any distinct pattern in all of these years, which strongly supports the concept of a ground-based network for uninterrupted observations with consistent duty cycles.

Finally, we present monthly and yearly duty cycles averaged over the entire period in Figure 18. We notice a mild trend in the monthly duty cycle (left panel of Figure 18) throughout the year reaching its lowest value in July (84 %) and the highest in December/January (91 %). We also notice a mild variation in the yearly values. The yearly mean is relatively low in the first two years and then remains around the mean over the entire period for rest of the years. The low standard deviations of 1.9 % and 2.2 % in monthly and yearly values, respectively exhibit excellent stability in the network duty cycle, even after more than 25 years of its operations. In addition, Figure 5 also indicates that there are no long-term changes in the duty cycles of any of the six network sites though the contribution from each site is affected by the local weather as well as the instrument down time. The lack of long-term variations in duty cycles further implies that there are no significant changes in climate in any of the GONG network sites. These findings clearly demonstrate that a ground-based network can reliably study long term solar variability.

The mean duty cycle over 18 years is 88.3 % and the median value is 92.0 %. Figure 19 displays the duty cycle corresponding to each day for the entire analysis period; smaller bars representing days where the duty cycle is lower than the median values. It is also observed that most days with lower duty cycles are around mid-year which is also apparent in monthly mean values displayed in Figure 18. Distribution of the daily values for bin-size of 2 % is given in Figure 20. We find that only 82 days out of 6574 days covered in this study have the duty cycle less than 50 %. Moreover, almost 13 % of the total days, i.e. 865 days, have a duty cycle of 99 % or greater of which 106 days have no gaps, i.e., 100 % duty cycle. In general, the frequency of occurrence gradually decreases with decreasing duty cycle except when values lie between 97 % –

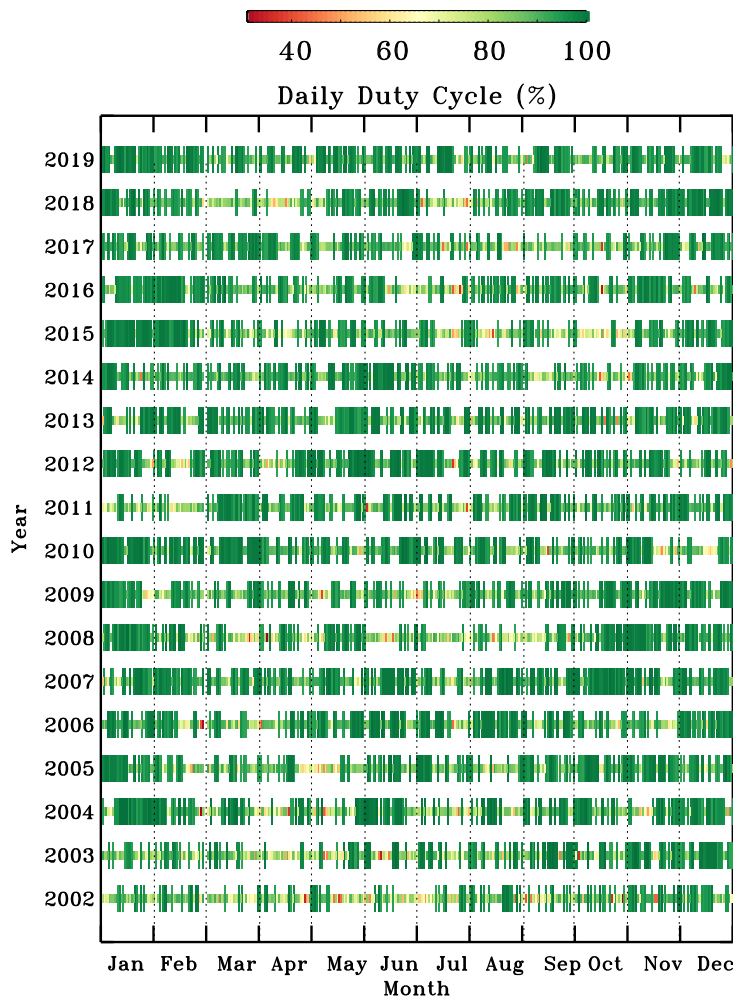


**Figure 19.** Daily duty cycle of GONG network for the entire period covered in this study, i.e. 2002–2019. Smaller bars represent days with duty cycle lower than the median value, i.e. 92 %.

98 % where we notice a slight increase.

It is important to mention that the above analysis is based on the *fully calibrated* images where each and every individual site image is passed through the pre-defined quality control checks (Clark et al. 2004). During this process, some images are rejected every day affecting the site as well as network duty cycles. To estimate the impact of the rejection criteria on the network duty cycle, we display the distribution of the duty cycle computed from the partially calibrated site images in Figure 21. Note that these partially calibrated images do not pass through all quality checks and may be counted for initial observations. A comparison between the duty cycles for partially and fully calibrated data reveals that the mean duty cycle obtained from the partially calibrated images is higher with the mean value of 93.5 % and the median value of 97 %. This is in excellent agreement with the GONG site-survey study where (Hill, Fischer,

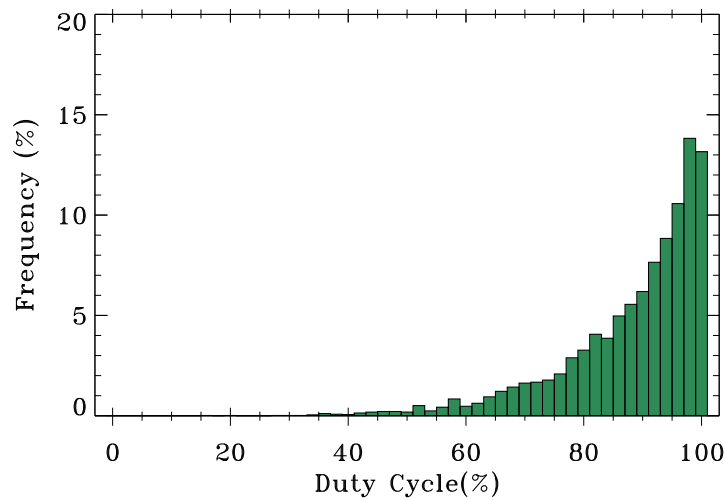


**Figure 20.** Histogram of daily duty cycle of the fully calibrated images for the entire period.

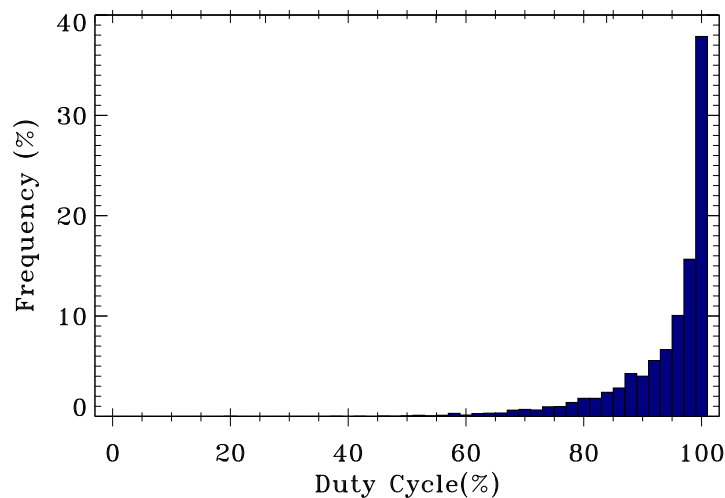


**Figure 21.** Distribution of daily duty cycle computed from all the images taken at sites. Please note that these images are partially calibrated (see text for explanation).

Forgach, Grier, Leibacher, Jones, Jones, Kupke, Stebbins, Clay, Ingram, Libbrecht, Zirin, Ulrichi, Websteri, Hieda, Labonte, Lu, Sousa, Garcia, Yasukawa, Kennewell, Cole, Zhen, Su-Min, Bhatnagar, Ambastha, Al-Khashlan, Abdul-Samad, Benkhaldoun, Kadiri, Sánchez, Pallé, Duhalde, Solis, Saá & González 1994) suggested an achievable duty cycle value of 93.3 %. This also indicates that the quality control matrices reduce the duty cycle by about 5 % on an average, however there are large number of days when the duty cycle is not affected in this process, primarily due to multiple-site observations for a given minute. Compared to fully calibrated data where only 13 % of the days have duty cycle 99 % or more, the partially calibrated data have about 40 % of the days with duty cycle in this range. This reduction in duty cycle is also seen in another six-site network, BiSON, where the duty cycle of 82 % reduces to 78 % when fully calibrated

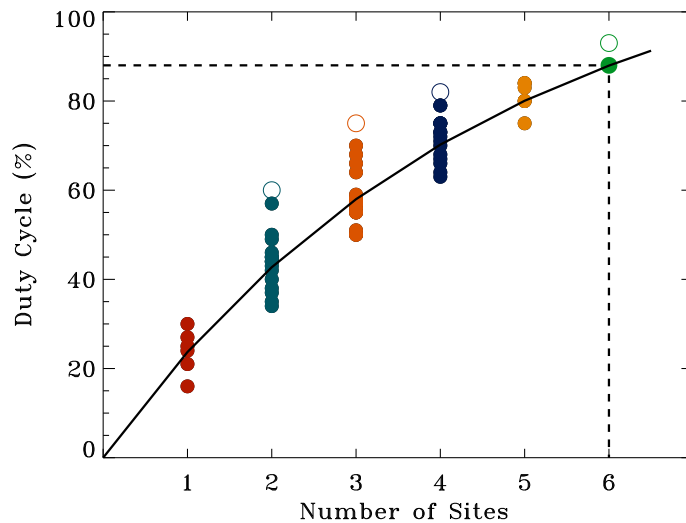


**Figure 22.** Dependence of the duty cycle on the number of sites. Filled circles represent values for each number of stations with different GONG-site combinations. Open circles are for the annual mean duty cycle computed using hypothetical networks as presented by (Hill & Newkirk 1985). Solid line represents fit to the data with a exponential function described in the text.

images were used (Hale et al. 2016).

### 5.1. Comparison with Previous Results

Based on the hypothetical networks, Hill & Newkirk (1985) reported that two-, three-, four-, and six-site networks might achieve 60 %, 75 %, 82 %, and 93 % annual mean duty cycle. To check the feasibility of these duty cycle values, we also computed duty cycles for all possible speculative networks using GONG’s fully calibrated site images and the results are displayed in Figure 22. The maximum duty cycles for two-, three-, four-, five-, and six-site combinations are 57 %, 70 %, 79 %, 84 %, and 88 %, respectively. These values are smaller by a few percent than those reported in Hill & Newkirk (1985). These are shown by the open symbols. It should be noted that the duty-cycle values obtained in this study are also affected by the downtime of each site due to instrument repairs and preventive maintenance trips which were not considered in the simulated analysis. However, as discussed earlier, the use of fully calibrated images reduces the duty cycle by about 5 % and thus the values obtained in this study are comparable with those reported by (Hill, Fischer, Forgach, Grier, Leibacher, Jones, Jones, Kupke, Stebbins, Clay, Ingram, Libbrecht, Zirin, Ulrichi, Websteri, Hieda, Labonte, Lu, Sousa, Garcia, Yasukawa, Kennewell, Cole, Zhen, Su-Min, Bhatnagar, Ambastha, Al-Khashlan, Abdul-Samad, Benkhaldoun, Kadiri, Sánchez, Pallé, Duhalde, Solis, Saá & González 1994).

To study the impact of number of sites on the duty cycle, we finally fit duty cycle values obtained for different site combinations to a function. The best fit is found for

**Table 5.** Multi-site simultaneous contribution to the network duty cycle.

Simultaneous Observations Type	Count [Minutes]	Duty Cycle	Details
Total	$4.24 \times 10^6$	44.84 %	
2 sites	$3.37 \times 10^6$	35.60 %	Table 6
3 sites	$8.20 \times 10^5$	8.66 %	Table 7
4 sites	$5.45 \times 10^4$	0.58 %	Table 8

an exponential function of the form of  $f(n) = -1.20e^{-0.22n} + 1.20$ , where  $f$  is the duty cycle, and  $n$  is the number of sites (Figure 22). It clearly displays that the duty cycle increases exponentially with the increasing number of sites, however the locations of the observing sites play a critical role in achieving desired duty cycle. We also find that adding another site to the six-site network will improve the duty cycle notably.

## 6. Simultaneous Observations from Multiple Sites

In a well-organized network, it is important that simultaneous observations are carried out at adjacent sites. This will not only minimize interruptions in observations but also helps in a better data calibration. In ideal conditions, the GONG network should be providing overlapping observations all of the time. However as presented in Table 2, almost 11 % of the period considered in this study was not covered by any site and the rest of the coverage was equally divided among single-site and overlapping observations. Table 5 illustrates the details of simultaneous observations from two, three, and four sites. As expected, the maximum simultaneous coverage comes from two-site overlap. This is in agreement with the site-survey study by (Hill, Fischer, Forgach, Grier, Leibacher, Jones, Jones, Kupke, Stebbins, Clay, Ingram, Libbrecht, Zirin, Ulrichi, Websteri, Hieda, Labonte, Lu, Sousa, Garcia, Yasukawa, Kennewell, Cole, Zhen, Su-Min, Bhatnagar, Ambastha, Al-Khashlan, Abdul-Samad, Benkhaldoun, Kadiri, Sánchez, Pallé, Duhalde, Solis, Saá & González 1994) where they also achieved a maximum overlap of 44.8 % between two sites. Further, the single-site observations were limited to 28.9 %, which is lower than this study, and three- and four-site simultaneous observations contributed to 18.5 % and 1.7 % of the total observing time.

### 6.1. Simultaneous Observations from Two Sites

Table 5 shows that the two-site simultaneous observations provide coverage of about 35.6 % over the entire period. We present in Table 6 the details of the two-site observations and their coverage. In addition, every site has some fraction of overlapping observations with adjacent sites. It can be easily seen that two-site observations provide coverage between 34 % – 56 %, however the simultaneous coverage ranges between <0.1 % and 7.3 %. It is obvious that the simultaneous coverage depends on the locations of the sites in the network. The maximum overlap is observed between two pairs of sites, i.e.,

**Table 6.** Simultaneous coverage from two sites in the network.

Site 1	Site 2	Total Coverage		Simultaneous Coverage	
		[Minutes]	Duty Cycle	[Minutes]	Duty Cycle
LE	UD	$3.2 \times 10^6$	34.4 %	$6.9 \times 10^5$	7.3 %
	TD	$4.8 \times 10^6$	50.5 %	$9.7 \times 10^4$	1.0 %
	CT	$5.4 \times 10^6$	56.8 %	211	<0.1 %
	BB	$4.6 \times 10^6$	49.0 %	$6.9 \times 10^4$	0.7 %
	ML	$4.1 \times 10^6$	43.8 %	$3.1 \times 10^5$	3.3 %
UD	TD	$3.6 \times 10^6$	38.4 %	$2.2 \times 10^5$	2.3 %
	CT	$4.3 \times 10^6$	45.9 %	$1.0 \times 10^4$	0.1 %
	BB	$3.7 \times 10^6$	39.5 %	34	<0.1 %
	ML	$3.5 \times 10^6$	36.7 %	$1.7 \times 10^4$	0.1 %
TD	CT	$4.2 \times 10^6$	44.8 %	$6.9 \times 10^5$	7.3 %
	BB	$4.2 \times 10^6$	44.0 %	$1.4 \times 10^5$	1.5 %
	ML	$4.3 \times 10^6$	45.2 %	$1.6 \times 10^4$	0.1 %
CT	BB	$4.0 \times 10^6$	42.4 %	$4.0 \times 10^5$	4.2 %
	ML	$4.1 \times 10^6$	43.5 %	$2.8 \times 10^5$	3.0 %
BB	ML	$3.3 \times 10^6$	34.9 %	$4.7 \times 10^5$	4.4 %

LE and UD, and TD and CT, with a contribution of 7.3 % to the total duty cycle. However, LE and UD have more overlapping observations, i.e., 21.6 % of their total coverage compared to TD and CT with an overlapping observation of 16.4 %.

### 6.2. Simultaneous Observations from Three Sites

Compared to two-site observations, three-site simultaneous coverage is less frequent and the contribution is about 8.66 % in the total duty cycle. Table 7 presents the coverage between three sites where we have included only those sites that observed simultaneously at any point in the entire period. We find only two three-site combinations that observed simultaneously for >1 % in the total coverage. Among these, the maximum overlap is obtained between CT, BB, and ML.

### 6.3. Simultaneous Observations from Four Sites

For a tiny fraction in network duty cycle, i.e. <1 % , four GONG sites observed simultaneously. As presented in Table 8, the maximum contribution came from TD, CT, BB, and ML. These sites covered 63 % of the available time together in 6574 days of which only 0.57 %, i.e. 54,423 min observed simultaneously. There are two other site combinations in this category, however their contribution to the network duty cycle is less than 0.01 %.



**Table 7.** Simultaneous coverage from three sites in the network.

Site 1	Site 2	Site 3	Total Coverage		Simultaneous Coverage	
			[Minutes]	Duty Cycle	[Minutes]	Duty Cycle
LE	UD	TD	$5.3 \times 10^6$	55.9 %	$5.4 \times 10^4$	0.6 %
LE	UD	ML	$4.9 \times 10^6$	51.4 %	$2.7 \times 10^4$	0.3 %
LE	CT	BB	$6.4 \times 10^6$	67.8 %	$2.0 \times 10^2$	<0.1 %
LE	CT	ML	$6.3 \times 10^6$	66.0 %	$3.9 \times 10^2$	<0.1 %
LE	BB	ML	$5.4 \times 10^6$	56.7 %	$4.4 \times 10^4$	0.5 %
UD	TD	CT	$5.5 \times 10^6$	57.7 %	$1.2 \times 10^4$	0.1 %
TD	CT	BB	$5.2 \times 10^6$	55.1 %	$2.4 \times 10^5$	2.5 %
TD	CT	ML	$5.5 \times 10^6$	57.6 %	$2.5 \times 10^4$	0.3 %
TD	BB	ML	$5.2 \times 10^6$	54.9 %	$3.9 \times 10^4$	0.4 %
CT	BB	ML	$4.8 \times 10^6$	50.4 %	$3.8 \times 10^5$	4.0 %

**Table 8.** Simultaneous coverage from four sites in the network.

Sites	Total Coverage		Simultaneous Coverage	
	[Minutes]	Duty Cycle	[Minutes]	Duty Cycle
LE, CT, BB, ML	$6.8 \times 10^6$	72.3 %	328	<0.01 %
LE, UD, BB, ML	$6.1 \times 10^6$	64.3 %	14	<0.01 %
TD, CT, BB, ML	$6.0 \times 10^6$	63.0 %	54423	0.57 %

## 7. Significance of High Duty Cycle

GONG’s uninterrupted full-disk observations have been widely used in numerous science projects as well as space-weather operations/monitoring where duty cycle plays a pivotal role. In particular, helioseismic studies have been greatly benefited from these long span of observations. For example, the continuous data with consistently high duty cycle have allowed the study of temporal variability in global (Jain et al. 2009, Jain et al. 2011, Broomhall 2017) as well as local oscillation mode characteristics (Tripathy et al. 2013, Tripathy et al. 2015) and their connection with the 11-year cyclic behaviour of the surface magnetic activity. In addition, these data have also revealed other periodicities in helioseismic data, e.g., the quasi-biennial oscillations (QBO) in oscillation frequencies (Simoniello et al. 2013). Further, long consistent helioseismic data are also crucial in constraining the fundamental stellar properties, particularly in asteroseismology where most stellar observations cover relatively short time intervals (Howe et al. 2020).

Another benefit of Doppler observations with high duty cycle is the reliable inferences of subsurface flows which are crucial in understanding the plasma motion below the surface and the solar dynamo. Several studies have been carried out where

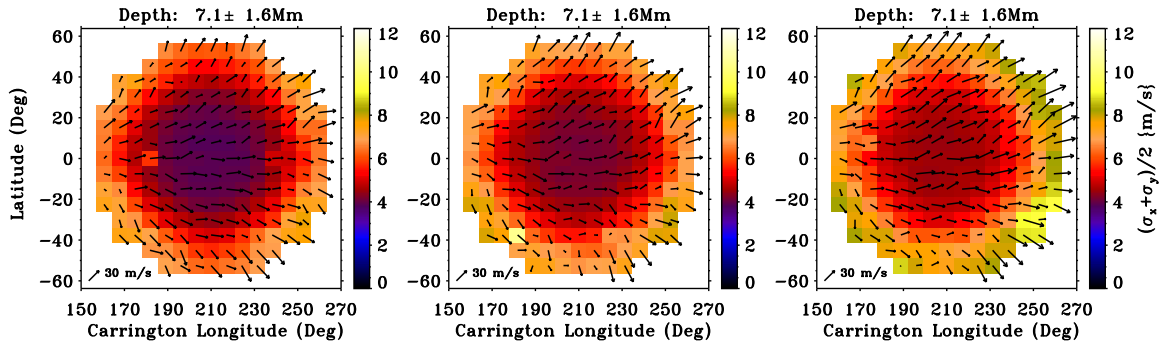


**Figure 23.** Effect of duty cycle on the subsurface flow measurements computed using 1664 min GONG Dopplergrams with (Left) 100%, (Middle) 79%, and 66% (Right) duty cycles. Arrows show the flow magnitude and the direction, and the background depict the uncertainties in these estimates.

torsional oscillation patterns (Howe et al. 2000, Howe et al. 2018), subsurface zonal and meridional flows (Komm et al. 2018, Basu & Antia 2019, Gizon et al. 2020), and deep meridional flows (Jackiewicz et al. 2015) have been reliably inferred. To emphasize the importance of high-duty cycle in helioseismic studies, we compare horizontal flows (Figure 23) computed utilizing the technique of ring diagrams (Hill 1988) where 1664 full-disk Doppler images taken at 1 min cadence are used. In the figure, arrows show the flow magnitude and the direction, and the background depict the uncertainties in these estimates. The left panel shows the horizontal flows with a 100% duty cycle while the middle and right panels display the flows measured with reduced duty cycles of 79% and 66%, respectively. Lower duty cycles are computed by truncating observations from 100% duty cycle data. From a comparison of these three panels, we notice that the flow magnitudes as well as the errors increase with the decrease of the duty cycles. Thus, the reliable flow measurements require a higher duty cycle.

GONG has also become an important data source for uninterrupted high-cadence magnetic-field and  $H\alpha$  observations, primarily due to significantly high duty cycle. These are being used in various space-weather forecast systems (Petrie et al. 2008, Arge et al. 2010) and the studies related to flare and filament eruptions (Luna et al. 2018). In addition, maps of the invisible-side (farside) of the Sun, computed from GONG Dopplergrams, identifying active regions before they rotate towards Earth are another important data product (González Hernández et al. 2007, González Hernández et al. 2010). An example of consequences of low-duty cycle in farside mapping is illustrated in Figure 24. Here we display farside maps for three different duty cycles using 24-h GONG observations for June 21, 2014. Top panel shows the map from 100% duty cycle as observed and other two panels display maps for lower duty cycles by artificially introducing gaps in the observations. It is clearly visible that reducing duty cycle reduces signal to noise and also increases random noise. It is also important to note that the uninterrupted synoptic observations are crucial in advancing our knowledge

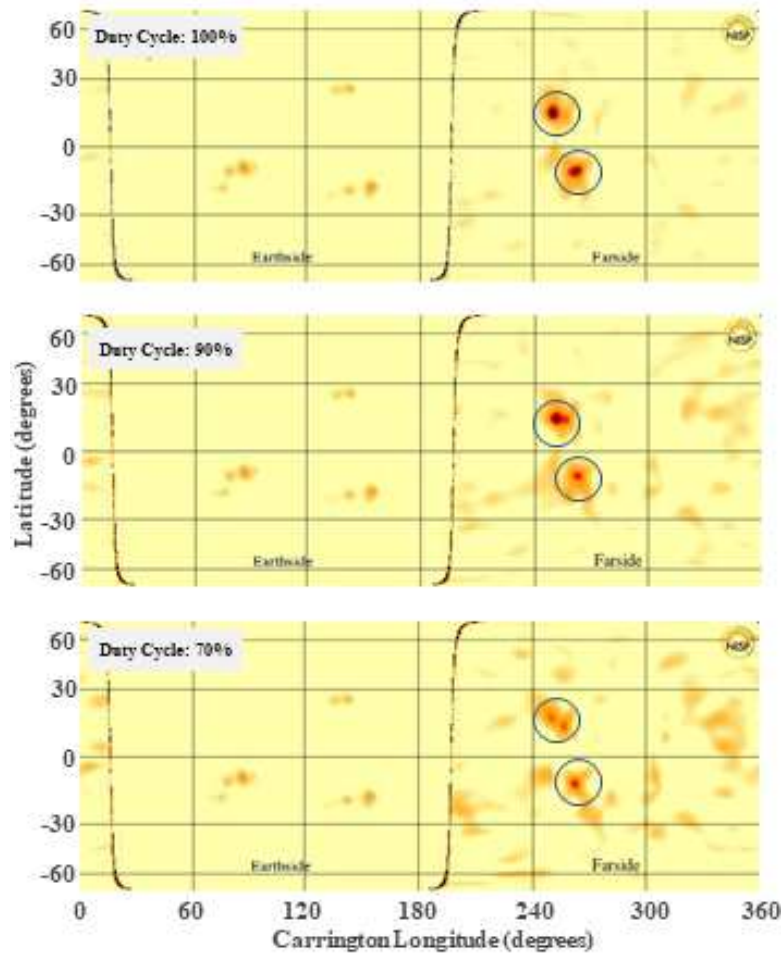


**Figure 24.** Effect of duty cycle on the farside helioseismic maps computed using 24 h GONG Dopplergrams with (top) 100 %, (Middle) 90 %, and (Bottom) 70 % duty cycles. Vertical lines show the boundaries between farside and nearside (direct observations) hemispheres. Regions of high magnetic field, i.e. active regions, are shown by the darker regions on both sides. Identified active regions on the farside are marked with circles. It is clearly visible that the low duty cycle increases noise in the farside maps and also reduces the signal to noise.

of the phenomena related to solar activity whose origin is still not fully understood (Elsworth et al. 2015).

## 8. Summary

Continuous observations of the Sun play an important role in the studies of long-term as well as short-term solar variability. In this context, GONG comprising of six ground-based observatories has been providing consistent and continuous observations spanning over more than two solar cycles with a stable temporal coverage. In this paper, we perform a detailed analysis of all the six sites and assess the duty cycle that has been achieved by individual as well as combined sites.

The study reveals that the maximum observations have been recorded at two sites located in the southern hemisphere and the lowest number of observations were obtained at the UD site, predominantly owing to the yearly site closure during the Indian monsoon. Further, there is significant overlap between observations from different sites, which is important for better calibration and for creating a seamless, long time series by merging observations from various sites. The mean and median duty cycle of the network is 88 % and 92 %, respectively,

Our study further demonstrates that strong seasonal trends are present at all sites except the Mauna Loa (ML) site, probably due to its geographical location. However, these trends disappear in the network when the observations from all sites are combined/merged. Although the down time of each site varies from year to year, we do not find long-term change in climate at any of the network sites that may affect the duty cycle.

It should be noted that the ground-based networks are less expensive as compared to space missions and have the ease of repairing/upgrading any instrument though the image quality might be affected by the atmospheric seeing. The detailed analysis presented here demonstrates that a significantly high duty cycle values can be achieved from a well-designed network of ground-based observatories and can provide an important platform for long-term synoptic observations.

## Acknowledgments

The authors would like to thank Jack Harvey, John Leibacher, and Charles Lindsey for critically reading the manuscript and their suggestions. K. Jain thanks Valentín Martínez Pillet for many useful discussions. GONG has received support from hundreds of people at the GONG headquarters at the National Solar Observatory and around the world, and their dedication is pivotal for maintaining the GONG operations for such a long time. The authors would like to thank all those who are, or have been, associated with GONG from its planning to the present. This work utilizes data from the National Solar Observatory Integrated Synoptic Program, which is operated by the Association of Universities for Research in Astronomy, under a cooperative agreement with the National Science Foundation and with additional financial support from the National Oceanic and Atmospheric Administration, the National Aeronautics and Space Administration, and the United States Air Force. The GONG network of instruments is hosted by the Big Bear Solar Observatory, High Altitude Observatory, Learmonth Solar Observatory, Udaipur Solar Observatory, Instituto de Astrofísica de Canarias, and the Cerro Tololo Interamerican Observatory.

## References

Arge C N, Henney C J, Koller J, Compeau C R, Young S, MacKenzie D, Fay A & Harvey J W 2010 *in* M Maksimovic, K Issautier, N Meyer-Vernet, M Moncuquet & F Pantellini, eds, ‘Twelfth

- International Solar Wind Conference' Vol. 1216 of *American Institute of Physics Conference Series* p. 343.
- Basu S & Antia H M 2019 *ApJ* **883**, 93.
- Broomhall A M 2017 *Sol Phys* **292**, 67.
- Chaplin W J, Elsworth Y, Howe R, Isaak G R, McLeod C P, Miller B A, van der Raay H B, Wheeler S J & New R 1996 *Sol Phys* **168**, 1.
- Chou D Y, Sun M T, Huang T Y, Lai S P, Chi P J, Ou K T, Wang C C, Lu J Y, Chu A L, Niu C S, Mu T M, Chen K R, Chou Y P, Jimenez A, Rabello-Soares M C, Chao H, Ai G, Wang G P, Zirin H, Marquette W & Nenow J 1995 *Sol Phys* **160**, 237.
- Clark R, Toner C, Hill F, Hanna K, Ladd G, Komm R, Howe R, Gonzalez-Hernandez I & Kholikov S 2004 in D Danesy, ed., 'SOHO 14 Helio- and Asteroseismology: Towards a Golden Future' Vol. 559 of *ESA Special Publication* ESA Noordwijk p. 381.
- Elsworth Y, Broomhall A M, Gosain S, Roth M, Jefferies S M & Hill F 2015 *Space Sci. Rev* **196**, 137.
- Finsterle W, Jefferies S M, Cacciani A, Rapex P, Giebink C, Knox A & Dimartino V 2004 *Sol Phys* **220**, 317.
- Fischer G, Hill F, Jones W, Leibacher J, McCurnin W, Stebbins R & Wagner J 1986 *Sol Phys* **103**, 33.
- Fossat E 1991 *Sol Phys* **133**, 1.
- Fossat E 2013 in K Jain, S. C Tripathy, F Hill, J. W Leibacher & A. A Pevtsov, eds, 'Fifty Years of Seismology of the Sun and Stars' Vol. CS-478 of *Astron. Soc. Pacific Conf. Ser* San Francisco p. 73.
- Gizon L, Cameron R H, Pourabdian M, Liang Z C, Fournier D, Birch A C & Hanson C S 2020 *Science* **368**, 1469.
- González Hernández I, Hill F & Lindsey C 2007 *ApJ* **669**, 1382.
- González Hernández I, Hill F, Scherrer P H, Lindsey C & Braun D C 2010 *Space Weather* **8**, 06002.
- Grec G, Fossat E & Pomerantz M 1980 *Nature* **288**, 541–544.
- Hale S J, Howe R, Chaplin W J, Davies G R & Elsworth Y P 2016 *Sol Phys* **291**, 1–28.
- Harvey J & GONG Instrument Team 1995 in R. K Ulrich, E Rhodes, Jr. & W Däppen, eds, 'GONG 1994. Helio- and Astro-Seismology from the Earth and Space' Vol. CS-76 of *Astron. Soc. Pacific Conf. Ser* San Francisco p. 432.
- Harvey J, Tucker R & Britanik L 1998 in S Korzenik, ed., 'Structure and Dynamics of the Interior of the Sun and Sun-like Stars' Vol. 418 of *ESA Special Publication* Noordwijk p. 209.
- Harvey J W 2013 in K Jain, S. C Tripathy, F Hill, J. W Leibacher & A. A Pevtsov, eds, 'Fifty Years of Seismology of the Sun and Stars' Vol. CS-478 of *Astron. Soc. Pacific Conf. Ser* San Francisco p. 51.
- Harvey J W, Bolding J, Clark R, Hauth D, Hill F, Kroll R, Luis G, Mills N, Purdy T, Henney C, Holland D & Winter J 2011 in 'AAS/Solar Physics Division Abstracts #42' Vol. 42 of *AAS/Solar Physics Division Meeting* p. 17.45.
- Harvey J W, Hill F, Hubbard R P, Kennedy J R, Leibacher J W, Pintar J A, Gilman P A, Noyes R W, Title A M, Toomre J, Ulrich R K, Bhatnagar A, Kennewell J A, Marquette W, Patron J, Saa O & Yasukawa E 1996 *Science* **272**, 1284–1286.
- Hill F 1988 *ApJ* **333**, 996.
- Hill F 2018 *Space Weather* **16**, 1488.
- Hill F, Bolding J, Clark R, Donaldson-Hanna K, Harvey J W, Petrie G J D, Toner C G & Wentzel T M 2008 in R Howe, R. W Komm, K. S Balasubramaniam & G. J. D Petrie, eds, 'Subsurface and Atmospheric Influences on Solar Activity' Vol. CS-383 of *Astron. Soc. Pacific Conf. Ser.* San Francisco p. 227.
- Hill F, Fischer G, Forgach S, Grier J, Leibacher J W, Jones H P, Jones P B, Kupke R, Stebbins R T, Clay D W, Ingram R E L, Libbrecht K G, Zirin H, Ulrich R K, Webster L, Hieda L S, Labonte B J, Lu W M T, Sousa E M, Garcia C J, Yasukawa E A, Kennewell J A, Cole D G, Zhen H, Su-Min X, Bhatnagar A, Ambastha A, Al-Khashlan A S, Abdul-Samad M S, Benkhaldoun Z, Kadiri S, Sánchez F, Pallé P L, Duhalde O, Solis H, Saá O & González R 1994 *Sol Phys* **152**, 351.
- Hill F, Fischer G, Grier J, Leibacher J W, Jones H B, Jones P P, Kupke R & Stebbins R T 1994 *Sol*

- Phys* **152**, 321.
- Hill F & Newkirk, Jr. G 1985 *Sol Phys* **95**, 201.
- Howe R, Chaplin W J, Basu S, Ball W H, Davies G R, Elsworth Y, Hale S J, Miglio A, Nielsen M B & Viani L S 2020 *Monthly Notices Royal Astron Soc* **493**, L49.
- Howe R, Christensen-Dalsgaard J, Hill F, Komm R W, Larsen R M, Schou J, Thompson M J & Toomre J 2000 *Science* **287**, 2456.
- Howe R, Hill F, Komm R, Chaplin W J, Elsworth Y, Davies G R, Schou J & Thompson M J 2018 *ApJL* **862**, L5.
- Jackiewicz J, Serebryanskiy A & Kholikov S 2015 *ApJ* **805**, 133.
- Jain K, Tripathy S C & Hill F 2009 *ApJ* **695**, 1567.
- Jain K, Tripathy S C & Hill F 2011 *ApJ* **739**, 6.
- Jefferies S M, Fleck B, Murphy N & Berrilli F 2019 *ApJL* **884**, L8.
- Komm R, Howe R & Hill F 2018 *Sol Phys* **293**, 145.
- Leibacher J & GONG Project Team 1995 in R. K Ulrich, E. J Rhodes, Jr. & W Däppen, eds, ‘GONG 1994. Helio- and Astro-Seismology from the Earth and Space’ Vol. CS-76 of *Astron. Soc. Pacific Conf. Ser.* San Francisco p. 381.
- Leibacher J W & Stein R F 1971 *Astrophys Lett* **7**, 191.
- Leighton R B 1960 in R. N Thomas, ed., ‘Aerodynamic Phenomena in Stellar Atmospheres’ Vol. 12 of *IAU Symp.* p. 321.
- Leighton R B, Noyes R W & Simon G W 1962 *ApJ* **135**, 474.
- Luna M, Karpen J, Ballester J L, Muglach K, Terradas J, Kucera T & Gilbert H 2018 *ApJS* **236**, 35.
- Pallé P L, Appourchaux T, Christensen-Dalsgaard J & Garc  a I A 2015 in V. C. H Tong & R. A Garc  a, eds, ‘Extraterrestrial Seismology’ Cambridge University Press p. 25.
- Petrie G J D, Bolding J, Clark R, Donaldson-Hanna K, Harvey J W, Hill F, Toner C & Wentzel T M 2008 in R. Howe, R. W Komm, K. S Balasubramaniam & G. J. D Petrie, eds, ‘Subsurface and Atmospheric Influences on Solar Activity’ Vol. CS-383 of *Astron. Soc. Pacific Conf. Ser.* San Francisco p. 181.
- Pintar J & Toussaint R 1998 in S Korzennik, ed., ‘Structure and Dynamics of the Interior of the Sun and Sun-like Stars’ Vol. 418 of *ESA Special Publication* p. 295.
- Simoniello R, Jain K, Tripathy S C, Turck-Chi  ze S, Baldner C, Finsterle W, Hill F & Roth M 2013 *ApJ* **765**, 100.
- Toner C G 2001 in A Wilson & P. L Pall  , eds, ‘SOHO 10/GONG 2000 Workshop: Helio- and Asteroseismology at the Dawn of the Millennium’ Vol. 464 of *ESA Special Publication* Noordwijk p. 355.
- Toner C G, Haber D, Corbard T, Bogart R & Hindman B 2003 in H Sawaya-Lacoste, ed., ‘GONG+ 2002. Local and Global Helioseismology: the Present and Future’ Vol. 517 of *ESA Special Publication* Noordwijk p. 405.
- Toussaint R, Harvey J & Hubbard R 1995 in R. K Ulrich, E. J Rhodes, Jr. & W D  ppen, eds, ‘GONG 1994. Helio- and Astro-Seismology from the Earth and Space’ Vol. CS-76 of *Astron. Soc. Pacific Conf. Ser.* p. 532.
- Tripathy S C, Jain K & Hill F 2013 *Sol Phys* **282**, 1.
- Tripathy S C, Jain K & Hill F 2015 *ApJ* **812**, 20.
- Ulrich R K 1970 *ApJ* **162**, 993.
- Woodard M F & Noyes R W 1985 *Nature* **318**, 449.